bioresources.com

Photocatalytic Degradation of Lignin Model Compounds and Kraft Pine Lignin by CdS/TiO₂ under Visible Light Irradiation

Wenzhi Li,[a] Mingjian Zhang,[a,b,]* Zhijie Du,[a] Qiaozhi Ma,[a] Hasan Jameel,[c] and Hou-min Chang [c]

Cadium sulfide/titanium dioxide (CdS/TiO₂) catalyst was prepared by two different methods: microemulsion-mediated solvothermal hydrolyzation (CdS/TiO₂ (SH)) and *in-situ* sulfurization under supercritical conditions (CdS/TiO₂ (SS)). The photocatalysts were characterized by nitrogen adsorption-desorption, X-ray diffraction, X-ray photoelectron spectra, UV-Vis absorption spectra, and PL spectra. Photodegradation reactions of three monomeric and one dimeric lignin model compounds, and kraft pine lignin (Indulin AT) were carried out at room temperature in a weak alkaline aqueous system by visible light irradiation with air bubbling. Quantitative results showed that these lignin model compounds and kraft lignin were effectively degraded. While both phenolic and non-phenolic lignin units are reactive, the phenolic units appeared to react faster and preferentially reacted.

Contact information: a: Department of Thermal Science and Energy Engineering, University of Science and Technology of China, Hefei 230026, China; b: Zhengzhou Tobacco Research Institute of China National Tobacco Corporation, Zhengzhou 450001, China; c: Department of Forest Biomaterials, North Carolina State University, Raleigh, NC 27695-8005, USA;
* Corresponding author: zmj119@mail.ustc.edu.cn

INTRODUCTION

As an important aromatic biopolymer and the second most abundant component in biomass, lignin provides a potentially rich resource of renewable mono-aromatic intermediates for high-value liquid fuels production (Fox *et al*. 2013). While lignin has been considered a major unfavorable component during conventional biochemical conversions of biomass to biofuels, *e.g.*, pyrolysis and hydrolysis, it accounts for more than 40% of the energy content of biomass (Mohan *et al*. 2006; Alvira *et al*. 2010). Thus, there is a strong need to develop an effective method for lignin utilization. However, the disordered and complex network of phenylpropanolic units results in a significant challenge of lignin conversion to the monophenolic products, which could be hydrogenated to alkanes with carbon numbers in the range of gasoline (Tuck *et al*. 2012). Many methods of catalytic lignin degradation have been developed to date, such as pyrolysis (Beis *et al*. 2010; Melligan *et al*. 2012; Brebu *et al*. 2013; Zhang *et al*. 2014), catalytic oxidation (Stärk *et al*. 2010; Voitl *et al*. 2010; Biannic and Bozell 2013), and catalytic reduction (Hartwig *et al*. 2012; Parsell *et al*. 2013). Some notable progress in lignin degradation has been made, *e.g.*, Voitl *et al.* (2010) obtained vanillin and methyl vanillate through catalytic oxidation in H_2O or $MeOH/H_2O$ mixtures with $H_3PMo_{12}O_{40}$. However, these lignin degradation

methods typically require elevated temperatures and pressures, which are adverse for active functional groups such as free phenols and γ-alcohols (Nguyen *et al*. 2013).

Photocatalysis, which is an advanced oxidation process (AOP), has been widely applied in water disinfection and organic compound decomposition. It provides a new potential technology for lignin degradation to produce renewable and low-molecular-weight monophenolic intermediates for liquid fuels under mild conditions (Li *et al*. 2008; Zakzeski *et al*. 2010; Costa and Alves 2013). The significant advantage lies in the use of a combination of biomass and solar energy, which is an alluring and promising route to generate monophenolic products with minimum energy consumption. Compared with the single-component photocatalysts, the coupled semiconductor system allows charge transfer between different components, which leads to efficient charge separation and minimizes unwanted electron-hole recombination. As a classic coupled semiconductor photocatalyst system, cadmium sulfide/titanium dioxide (CdS/TiO_2) has already attracted much attention for its excellent performance using visible light (Mali *et al*. 2008; Qian *et al*. 2011; Higashimoto *et al*. 2013). Most publications concerning lignin photocatalytic degradation are based on UV systems (Ma *et al*. 2008) or organic solvent systems (Tucker *et al*. 2011; Nguyen *et al*. 2013), with the disadvantage that these methods cannot effectively utilize the visible light of solar irradiation or require extra costs of organic solvents. Although some visible-light-active photocatalysts (Larraufie *et al*. 2011; Tucker *et al*. 2011) have exhibited excellent performance on dimeric model compounds linked with a typical C-O bond, a generalized visible light-mediated photocatalytic degradation of real lignin systems has not yet been reported, based on research into the topic.

In this paper, an attempt was made to establish a lignin degradation strategy that involved two kinds of CdS/TiO_2 photocatalysts and a weak alkaline aqueous system. Although only 7% of solar energy is composed of UV light, almost half of the solar energy is provided by visible light (Nah *et al*. 2010). Therefore, this visible-light photocatalytic system could utilize a much larger percentage of solar irradiation than current UV systems. In addition, an aqueous solution is a simple and low-cost system, which is beneficial for the separation of the final products. Because β-O-4 linkages comprise more than 50% of all the linkages found in lignin (Wu *et al*. 2012), photocatalytic degradation of a dimeric model compound with β-O-4 linkage and three mono-phenol model compounds was investigated under visible-light irradiation in pH 9.0 aqueous solutions with bubbling air. Photocatalytic degradation of kraft pine lignin is also discussed in this paper.

EXPERIMENTAL

Materials

Commercial TiO_2 P25 was purchased as a reference photocatalyst from Degussa (Germany).

Three mono-phenol model compounds, *i.e.*, 4-propylphenol (Alfa Aesar (USA), 98%), isoeugenol (Alfa Aesar, 98%), and 4-allyl-2,6-dimethoxyphenol (Alfa Aesar, 98%), were respectively denoted model compounds 1, 2, and 3. A β-O-4 dimer, 2-(2-methoxyphenoxy)-1-(3, 4-dimethoxy)phenyl-1, 3-propanediol (model compound 4), was synthesized using a method from previously published literature (Buendia *et al*. 2011). Indulin AT, a kraft pine lignin, was obtained from MeadWestvaco Co. (USA).

Other analytical reagents were purchased from Sinopharm Chemical Reagent Co. Ltd (China).

bioresources.com

Methods

Highly dispersed and stable CdS/TiO$_2$ (SH) and CdS/TiO$_2$ (SS) were prepared, respectively, by microemulsion-mediated solvothermal hydrolyzation and *in-situ* sulfurization under supercritical conditions (Wang *et al*. 2006; Huo *et al*. 2011).

CdS/TiO$_2$ (SH)

Cyclohexane (75.6 g), Triton X-100 (9.0 g), 1-hexanol (5.7 g), and 1 mL of deionized water were added to obtain a microemulsion under stirring conditions. Tetrabutyl titanate (3.0 g) was dropped into the above microemulsion with ultrasonic irradiation and vigorous agitation. After addition of the components, the microemulsion was reacted for 30 min to obtain hydrolyzed tetrabutyl titanate in water nanodroplets. Then, 3.5 mL of 0.3 M Cd(NO$_3$)$_2$ solution (Cd/Ti= 12 mol%) and 7.0 mL of 17 wt.% (NH$_4$)$_2$S aqueous solution were added dropwise into the mixture. Subsequently, the microemulsion was stirred for 48 h at room temperature. During this process, CdS nanoparticles were incorporated into TiO$_2$ colloids in the water nanodroplets. Afterwards, 250 mL of absolute ethanol and 300 mL of deionized water were added. The yellow precipitate obtained was separated by centrifugation and then thoroughly washed with deionized water. The final precipitate was dried in a vacuum at 313 K for 24 h. Finally, the yellow photocatalyst was identified as CdS/TiO$_2$ (SH).

CdS/TiO$_2$ (SS)

A mixture of 2.5 mL of 1.0 M HNO$_3$ and 10 mL of ethanol was added dropwise into a mixed solution of 10 mL of tetrabutyl titanate and 40 mL of ethanol at 313 K, followed by stirring for 60 min and aging for 48 h to obtain a TiO$_2$ xerogel. Then, the TiO$_2$ xerogel, 250 mL of ethanol, 1.08 g of Cd(NO$_3$)$_2$·4H$_2$O, and 0.268 g of (NH$_2$)$_2$CS were added into a 500-mL pressurized reactor under a nitrogen atmosphere. After being treated under supercritical conditions (553 K and 13.5 MPa) for 2 h, the system was rapidly cooled down to room temperature using a cold water jacket and the vapor was released slowly under a nitrogen atmosphere. Subsequently, the precipitate was obtained by filtration. The resulting solid was calcined in air at 623 K for 4 h, then calcined in a nitrogen atmosphere at 723 K for 5 h. The final product was identified as CdS/TiO$_2$ (SS).

Characterization of catalyst

The BET surface area (S_{BET}), the total pore volume (V_{pore}), and the average pore diameter (d_{pore}) of the photocatalysts were determined by the nitrogen adsorption-desorption isotherms, which were measured at 77 K on a Micromeritics TriStar II 3020 V1.03 apparatus (USA). Prior to the measurement, each sample was transferred to a glass adsorption tube and simultaneously degassed at 353 K under vacuum condition for 6 h. The photocatalyst structures were determined by X-ray diffraction (XRD; Philips X'Pert, The Netherlands) using Cu Kα radiation (wavelength = 0.154 nm). The surface Cd/Ti atomic ratios were determined by X-ray photoelectron spectroscopy (XPS) on a Thermo VG Scientific ESCALAB 250 (Thermo Scientific, USA), while the bulk Cd/Ti atomic ratios were determined using ICP-AES (Optima 7300 DV; Perkin Elmer Co., USA). The light absorption abilities of the photocatalysts were analyzed by photoluminescence spectra (PLS; JY Fluorolog-3-Tou, Horiba Scientific, USA) and UV-Vis diffuse reflectance spectra (DRS; SOLID3700, Shimadzu Co., Japan).

Photocatalytic degradation

Photocatalytic degradation experiments of model compounds 1, 2, 3, 4, and kraft pine lignin were carried out at room temperature in a cylindrical quartz reactor (5 cm in diameter). This reactor contained 25 mg of photocatalyst and 40 mL of pH 9.0 sodium hydroxide aqueous solutions with 1.0 mM of model compound 1, 2, 3, or 4, or 0.625 g/L of kraft pine lignin. The solutions were transparent, and no suspension was found. During the photodegradation of kraft pine lignin, 5 mg of n-heptanol was used as an antifoaming agent (Arnaudov *et al*. 2000). A 500-W Xenon lamp was positioned 20 cm away from the reactor to simulate solar light. The lamp was equipped with a circulating cooling water jacket (Pyrex) to eliminate the heating effect of far-infrared radiation. A cutoff filter was used to completely block the UV light (with a wavelength less than 420 nm) to ensure that the photocatalytic reactions were initiated by visible light. Diffusion limitations were minimized by stirring at 500 rpm. Air was bubbled at 15 mL/min to maintain air-equilibrated conditions for the photocatalytic system. The adsorption tests of model compounds 1, 2, 3, 4, and kraft pine lignin were conducted under the same conditions without light irradiation, and the degradation rates were calculated without the effect of adsorption.

A 5-mL sample of the mixture was obtained every 12 h during the reactions. The aqueous solution was then separated from the solid catalyst by centrifugation, and the pH was adjusted to 2.0 by dropwise addition of 0.3 M hydrochloric acid. The residual lignin was obtained by centrifugation and dried in a vacuum at 353 K for 24 h. Meanwhile, the liquid sample was extracted three times with 5 mL of ether. The combined ether solution was evaporated to a volume of 5 mL at room temperature under reduced pressure of about 3,000 Pa. The final ether sample was analyzed by gas chromatography/mass spectrometry (GC/MS) using a Shimadzu QP2010S mass selective detector and an Rtx-5MS capillary column (30 m × 250 μm × 0.25 μm). The injector temperature was set at 300 °C. The carrier gas was helium. The oven temperature program started at 40 °C (held for 3 min), ramped to 180 °C at a rate of 4 °C min^{-1}, and then ramped to 280 °C (held for 10 min) at a rate of 10 °C min^{-1}. The solvent delay of the mass spectrometer was 3 min. The identification of the chromatographic peaks of the compounds was achieved based on the NIST 2005 MS library. Quantitative analyses of identified photodegradation products and model compounds of lignin were made with benzaldehyde as the internal standard.

Kraft pine lignin and corresponding residual lignins were analyzed by Fourier transform infrared (FTIR) spectroscopy, ultraviolet/visible (UV/Vis) spectroscopy, and nuclear magnetic resonance (NMR). For FTIR analysis, the lignin sample (5 mg) was thoroughly mixed with 100 mg of KBr and the mixture was pressed into a pellet in a pellet die. The FTIR spectra were recorded between 400 and 4000 cm^{-1} at a resolution of 2 cm^{-1} using a Nicolet 8700 spectrometer (Fisher Scientific, USA).

The UV-Vis absorption spectra of the lignin solutions (original lignin, reduced lignin, reduced and ionized lignin solutions) were recorded on a SolidSpec-3700 spectrophotometer (Shimadzu) at room temperature. The stock solution of lignin was prepared by dissolving 5 mg of lignin in 10 mL of 70% dioxane solution. The stock solution (1 mL) was carefully transferred to a 10-mL volumetric flask and diluted to 10 mL with 50% dioxane (original lignin solution). For the reduced lignin solution, the stock solution (1 mL) was transferred to a 10-mL volumetric flask. Approximately 4 to 5 mg of sodium borohydride was added to the solution to reduce the α-carbonyl over 20 h, and it was acidified with 0.2 N HCl to pH 7.0. Finally, the obtained solution was diluted to 10 mL with 50% dioxane solution (reduced lignin solution). The spectra of reduced lignin were

measured by the UV/Vis at 305 nm. The α-carbonyl content was calculated based on the different absorbance at 305 nm between the original lignin solution and the reduced lignin solution. The extinction coefficient value at 305 nm is 9400 L mol^{-1} cm^{-1}. The reduced lignin solution was ionized with a sodium hydroxide pellet to pH 13 (reduced and ionized lignin solution). The calculations of free phenolic hydroxyl and stilbene moieties were based on the different absorbance between the reduced and ionized lignin solution and the reduced lignin solution at 300 nm and 378 nm, respectively. The extinction coefficient values at 300 nm and 378 nm are 4100 L mol^{-1} cm^{-1} and 24,300 L mol^{-1} cm^{-1}, respectively.

The NMR spectra were recorded on a Bruker AVANCE 400 MHz spectrometer (Germany) at 300 K using approximately 60 mg/mL lignin sample solutions in dimethyl-d6 sulfoxide. Chemical shifts were referenced to the residual DMSO signal (2.5/39.5). The conditions for the heteronuclear singular quantum correlation (HSQC) analysis were as follows: 90° pulse width of 13.4 μs, 1.46 s pulse delay (d1), and acquisition of 176 data points using a 5-mm BBO probe head (BB/^{1}H). ^{13}Carbon NMR employed a 90° pulse width of 11.8 μs, an acquisition time of 1.36 s, and a 2.0-s relaxation delay using a 5-mm BBO probe head (BB/^{1}H). A total of 20,480 scans *per* sample were collected.

RESULTS AND DISCUSSION

Photocatalytic Degradation

Lignin is a three-dimensional polymer that is composed of p-hydroxyphenyl- (H), guaiacyl- (G), and syringyl-propane (S) type monomeric units (Chen *et al.* 2011). Hence, 4-propylphenol (H, model compound 1), isoeugenol (G, model compound 2), and 4-allyl-2, 6-dimethoxyphenol (S, model compound 3) were used to explore the effect of lignin monomer type on the photodegradation process. The degradation rates at various reaction times are shown in Fig. 1.

The results revealed that the three model compounds of lignin monomers could be efficiently degraded using both photocatalysts at ambient temperature under visible light irradiation. Under the same photocatalytic degradation conditions, the type of monomeric units had a significant influence on the photodegradation rate. The degradation rate of lignin monomer compound 2 (G-type) was apparently higher than that of lignin monomer compound 3 (S-type), while lignin monomer compound 3 (S-type) degraded faster than lignin monomer compound 1 (H-type). The slower rate of reaction of the H model compound may be attributed to the lack of conjugated double bonds and/or the difference of substituents on the benzene ring. Furthermore, no degradation products of lignin monomer compounds 1-3 could be detected by GC/MS, presumably because of the much faster reaction rates of the initial reaction products and low concentrations of the model compounds in aqueous solution. CdS/TiO$_2$ (SH) showed higher photodegradation rates than those of CdS/TiO$_2$ (SS) for all three model compounds of lignin monomers under the same conditions.

The β-O-4 linkage is the most common type of C-O bond in the lignin biopolymer (Wu *et al*. 2012). 2-(2-methoxyphenoxy)-1-(3, 4-dimethoxy)phenyl-1, 3-propanediol (model compound 4) was studied as a β-O-4 model compound of lignin dimer. The proposed photodegradation scheme of lignin dimer compound 4 is shown in Scheme 1. Its degradation rates and the yields of corresponding products are shown in Fig. 2.
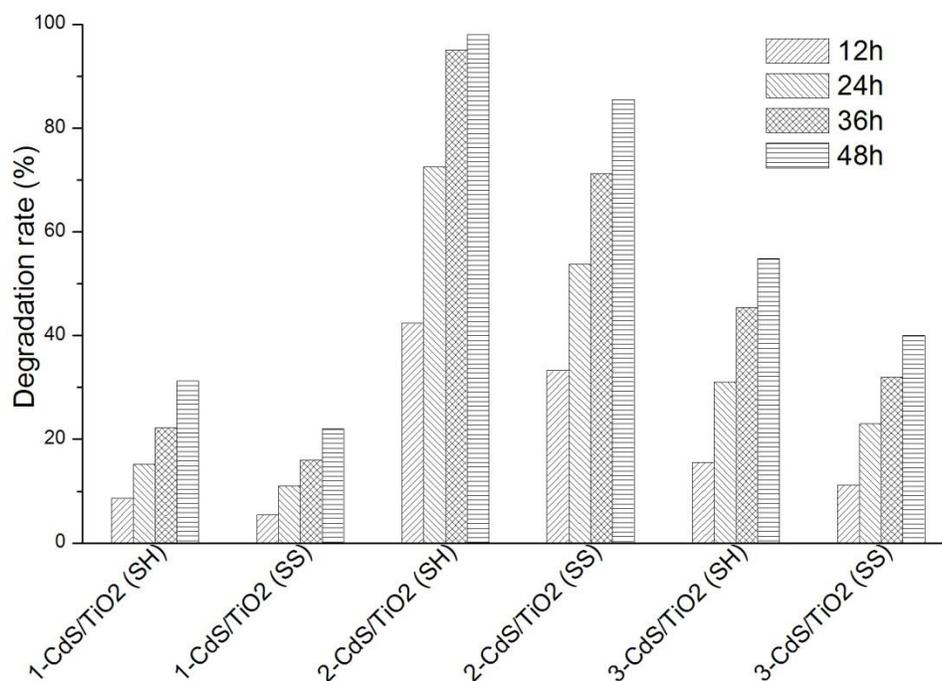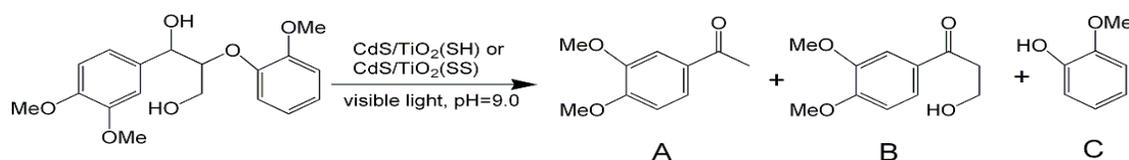
Fig. 1. The degradation rates of lignin monomer compounds 1, 2, and 3. Conditions: initial pH = 9.0, 0.625 g/L catalyst, 1.0 mM lignin monomer compound 1, 2, or 3, 15 mL/min air bubbling, ambient temperature

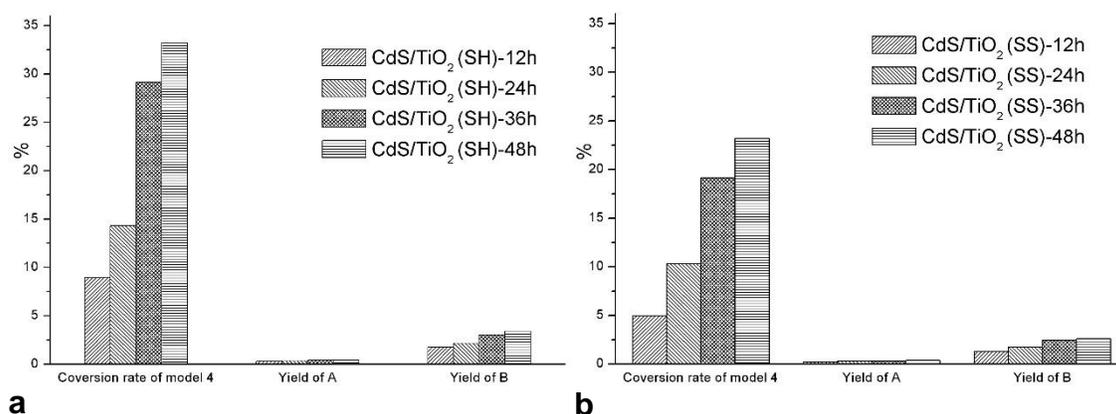**Scheme 1.** Photodegradation reaction of lignin dimer compound 4

Fig. 2. The degradation rates of lignin dimer 4 and yields of degraded products. (a) CdS/TiO$_2$ (SH) and (b) CdS/TiO$_2$ (SS). Conditions: initial pH = 9.0, 0.625 g/L CdS/TiO$_2$ (SH) or CdS/TiO$_2$ (SS), 1.0 mM lignin dimer compound 4, 15 mL/min air bubbling, ambient temperature

Appearance of the corresponding products A (3, 4-dimethoxyacetophenone) and B (1-(3, 4-dimethoxyphenyl)-3-hydroxy-1-propanone) confirmed that a benzylic oxidation

was introduced upon the α-carbon; $C_β$-$C_γ$ and β-O-4 ether bond cleavage occurred in our photodegradation system. The expected product C (guaiacol G-type) could not be detected, possibly because of a much faster reaction rate of further degradation to CO_2 and H_2O, which was consistent with the photodegradation results of lignin monomers 1-3 described above.

The degradation rate of model compound 4 was much lower than that of model compound 2 by both catalysts, suggesting that the mono-phenolic unit was more reactive than the non-phenolic unit under the photodegradation system employed. Nevertheless, the results clearly indicated that both phenolic and non-phenolic moieties in lignin were degraded under the system studied in this paper. The results also indicated that the catalytic activity of CdS/TiO_2 (SH) was higher than that of CdS/TiO_2 (SS) for the photo-degradation of lignin model compounds under visible light irradiation.

Photodegradation of Kraft Pine Lignin

Kraft pine lignin is only composed of linked guaiacyl-type (G) monomer units. Photocatalytic degradation of kraft pine lignin was conducted to evaluate the performance of CdS/TiO_2 (SH) and CdS/TiO_2 (SS) at room temperature in an alkaline aqueous system. After 48 h of reaction with CdS/TiO_2 (SH) and CdS/TiO_2 (SS), only 76% and 87% kraft pine lignin, respectively, were recovered when the reaction mixtures were acidified to pH 2, suggesting substantial oxidative degradation of kraft pine lignin. Degradation products from the photocatalytic degradation of kraft pine lignin were analyzed using qualitative GC/MS, and the typical GC/MS ion chromatogram of degraded products from kraft pine lignin is shown in Fig. 3.
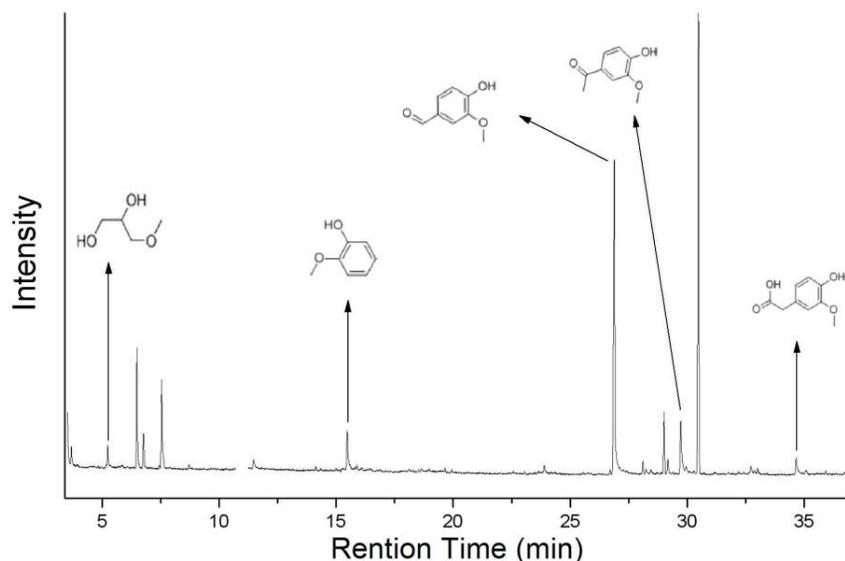

Fig. 3. Typical GC/MS chromatograph of the photodegradation products of kraft pine lignin. Conditions: initial pH = 9.0, 0.625 g/L CdS/TiO_2 (SH), 0.625 g/L kraft pine lignin, 15 mL/min air bubbling, ambient temperature. The peak between 10.70 and 11.25 min, which represents 1-heptanol, and was not collected

Among the degradation products, guaiacol, vanillin, apocynin, homovallinic acid, and 3-methoxy-1,2-propanediol were identified. The quantitative analysis of the photodegradation products is shown in Fig. 4. The major product from photodegradation

of kraft pine lignin was vanillin. However, the yields of degradation products were extremely low. The maximum concentration of vanillin by CdS/TiO$_2$ (SH) was 0.002 mM (or 0.00028 g/L), which amounts to less than 0.1% of the lignin. The low yield of degradation products is not due to adsorption on the two catalysts, as no significant carbon species were detected by XPS on two fresh photocatalysts. Thus, the low yield is most likely due to the fact that degradation products are much more reactive than kraft pine lignin. The detection of these degradation products, albeit in small yield, suggest that the degradation of kraft pine lignin is similar to that of the model compounds described above. The detection of 3-methoxy-1, 2-propanediol points to a possible ring-opening reaction.
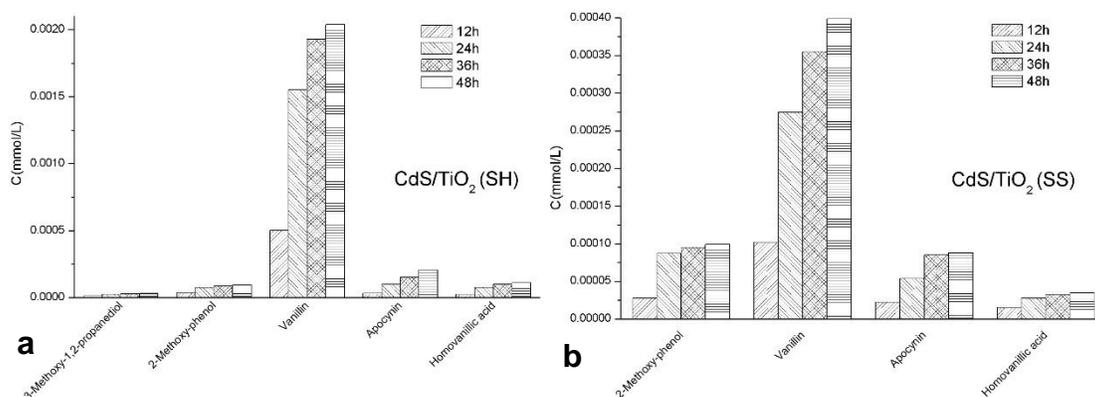

Fig. 4. Concentrations of degradation products of kraft pine lignin under visible light irradiation. (a) CdS/TiO$_2$ (SH) and (b) CdS/TiO$_2$ (SS). Conditions: initial pH = 9.0, 0.625 g/L CdS/TiO$_2$ (SH) or CdS/TiO$_2$ (SS), 0.625 g/L kraft pine lignin, 15 mL/min air bubbling, ambient temperature
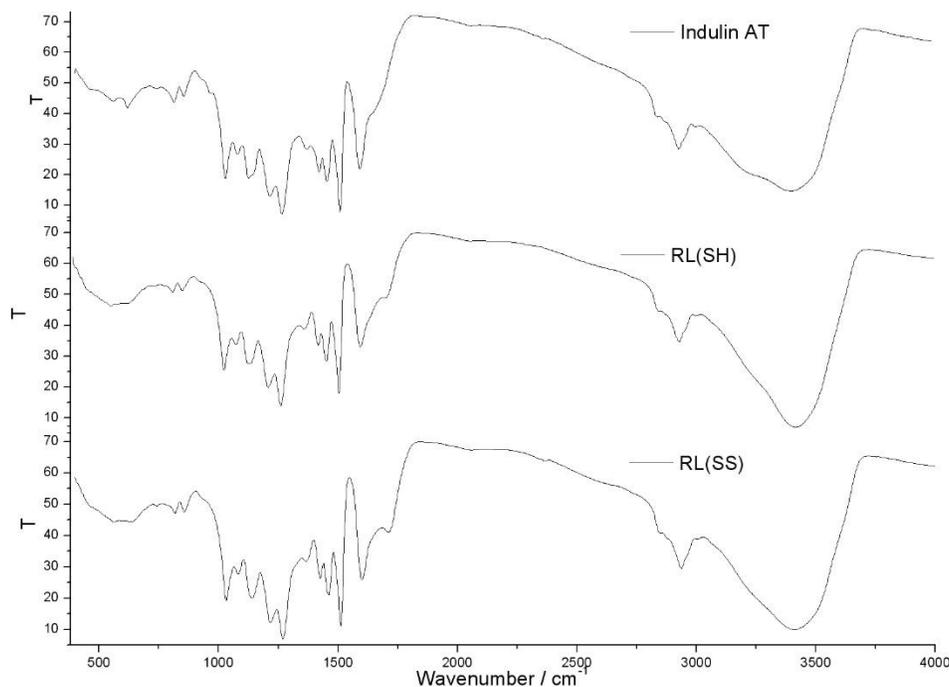

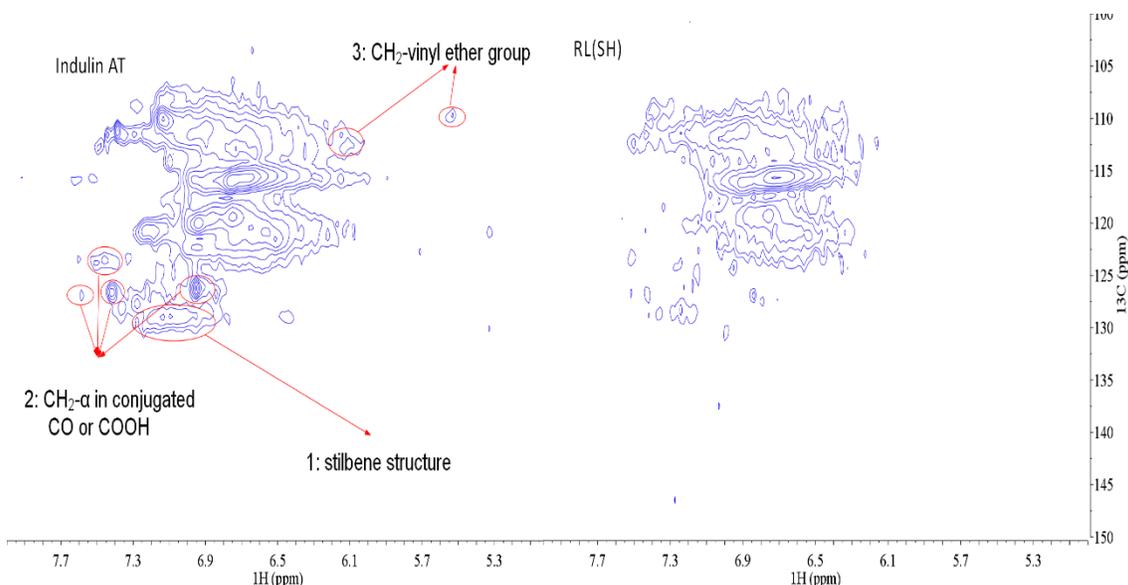**Fig. 5.** FTIR spectra of residual lignin and kraft pine lignin

Fig. 6. 2D-HSQC NMR spectra of kraft pine lignin and RL (SH)

The 76% and 87% of kraft pine lignin recovered after 48 h of reaction with CdS/TiO$_2$ (SH) and CdS/TiO$_2$ (SS), respectively, are of interest, as these photocatalytic degradation methods may be low-cost ways to modify kraft lignin for potential biomaterial applications. A preliminary characterization was carried out for these residual lignins, which are referred to as RL (SH) and RL (SS) for reactions with CdS/TiO$_2$ (SH) and CdS/TiO$_2$ (SS), respectively. The FTIR spectra of the two residual lignins, along with that of the original kraft pine lignin, are shown in Fig. 5. The three spectra are very similar, clearly indicating that the residual lignins retain their aromatic softwood lignin structures.

An ultraviolet (UV) spectral method was used to determine the functional group contents of residual lignin. Phenolic hydroxyl content and stilbene structure were determined by an ionization difference ($\Delta\varepsilon_i$) spectrum after reduction with sodium borohydride, whereas α-carbonyl content was determined by a reduction difference spectrum ($\Delta\varepsilon_r$). Originally, kraft pine lignin has a phenolic hydroxyl content of 48%, a stilbene content of 5.6%, and an α-carbonyl content of 9.4%, all based on 100 aromatic nuclei. After the photocatalytic reactions, the phenolic hydroxyl content decreased by 45% and 34%, the stilbene structure decreased by 44% and 34%, and the α-carbonyl content decreased by 46% and 43% for RL (SH) and RL (SS), respectively, suggesting preferential reaction of these functional groups. These results are confirmed by comparing the 2D-HSQC NMR spectra of kraft pine lignin and the residual lignins. The aromatic carbon/hydrogen portion of the spectra are shown side by side in Fig. 6 for kraft pine lignin and RL (SH). As can be seen, the signal associated with the stilbene structure (128/7.0-7.3) and the signals associated with an aromatic C-H bond conjugated with an α-carbonyl group or an α-carboxyl group (126.2/7.0; 123.6/7.5; 126.6/7.4 and 126.8/7.6) are almost absent in the spectrum of RL (SH). In addition, the two signals associated with a vinyl ether group (109/5.5 and 112/6.1) are also absent in the spectrum of RL (SH), indicating that vinyl ether is also preferentially reacted in the photocatalytic system. Similar results are also observed in the spectrum of RL (SS).

The stilbene and vinyl ether structures are known to be formed during the kraft pulping process through the quinone methide intermediate and the presence of free

phenolic hydroxyl groups is a prerequisite of their formation. The decrease in phenolic hydroxyl content and the disappearance of stilbene and vinyl ether clearly indicates that units with free phenolic hydroxyl groups are preferentially reacted. This result is consistent with the results of the model compounds discussed earlier, that demonstrated compounds with free phenolic hydroxyl groups react much faster than etherified model compounds.

Structure Parameters of Photocatalysts

The XRD measurements were carried out to determine the crystal phase composition of the two photocatalysts. As shown in Fig. 7, the XRD patterns confirmed that the TiO_2 was anatase (JCPDS 21-1272) and CdS had a cubic phase (JCPDS 80-19) in both photocatalysts. The peaks of 25.2°, 38.0°, 48.1°, 54.1° and 62.8° were regarded as an attributive indicator of anatase phase TiO_2 (101), (103, 004, and 112), (200), (105), and (204), respectively. Meanwhile, the additional peaks of 27.5°, 43.9° and 55.1° can be assigned to the CdS cubic phase (111), (220), and (222) crystal planes, respectively.

Structure parameters of the two photocatalysts are shown in Table 1. As the composite structure of CdS/TiO_2 (SH) and CdS/TiO_2 (SS) were confirmed by previous published studies (Wang *et al.* 2006; Huo *et al.* 2011), the further comparison of the two photocatalysts was conducted in this work. With around 15 wt.% loading of Cd, the BET surface area and surface Cd/Ti atomic ratio of CdS/TiO_2 (SH) were much larger than those of CdS/TiO_2 (SS), which improved photodegradation activity under visible light irradiation. The UV-Vis absorption spectra of the two CdS/TiO_2 composites and pure TiO_2 (P25) are shown in Fig. 8, which revealed that the absorptions of both CdS/TiO_2 composites were extended to the visible region with an apparently enhanced absorption between 400 and 500 nm compared to that of P25. It was clearly shown that the improvement of visible-light-absorbing efficiency was achieved for both coupled CdS/TiO_2 composites. Compared to CdS/TiO_2 (SS), CdS/TiO_2 (SH) had a larger absorption intensity in the wavelength range of 400 nm and 500 nm, which was obviously favorable for photodegradation under visible light.
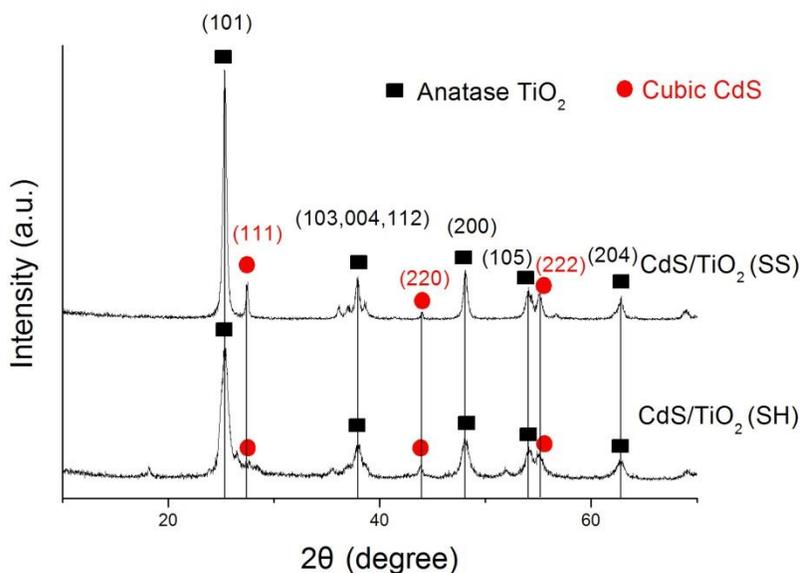

Fig. 7. XRD patterns of CdS/TiO_2 (SH) and CdS/TiO_2 (SS)

The efficient charge transfer from the CdS conduction band to the TiO_2 conduction band in CdS/TiO_2 composites could enhance charge density in the TiO_2 conduction band, and photo-induced electrons were effectively separated from holes in the CdS semiconductor to inhibit the recombination of electrons and holes (Wang *et al.* 2006; Huo *et al.* 2011). As shown in Fig. 9, the PL spectrum of CdS/TiO_2 (SH) exhibited weaker peak intensity at 530 nm than that of CdS/TiO_2 (SS), leading to a lower charge combination probability (Huo *et al.* 2011; Peng *et al.* 2013). Consequently, the utilization efficiency of photo-induced electron-hole pairs for CdS/TiO_2 (SH) was higher compared to that of CdS/TiO_2 (SS).

Table 1. Structure Parameters and Photoactivities of Two Photocatalysts

Sample	S_{BET} * (m^2 g^{-1})	V_{pore} * (cm^3 g^{-1})	d_{pore} * (nm)	Cd/Ti (mol %)		Degradation rate of kraft pine lignin (wt.%)
				Bulk	Surface	
CdS/TiO_2 (SH)	104	0.098	3.1	13.2	71.2	24.1
CdS/TiO_2 (SS)	56	0.199	13.2	12.7	57.5	12.6
P25	50	0.200	21	- **	-	-

* S_{BET}, V_{pore}, and d_{pore} are abbreviations of the BET surface area, the total pore volume, and the average pore diameter, respectively
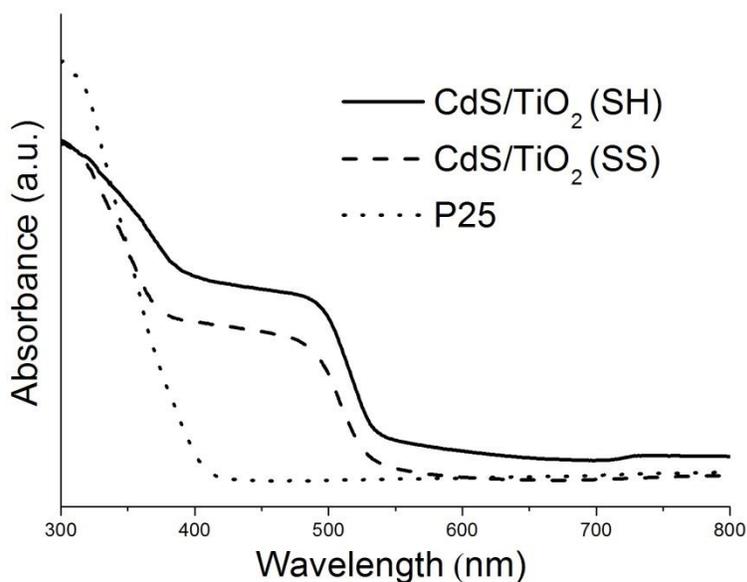** data is null

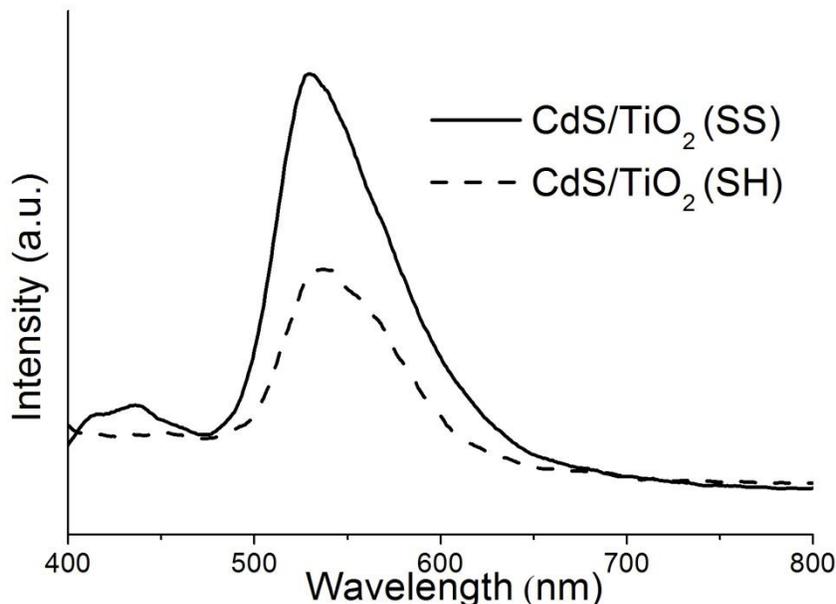**Fig. 8.** UV-Vis absorption spectra of CdS/TiO_2 (SH), CdS/TiO_2 (SS), and P25

Fig. 9. PL spectra of CdS/TiO$_2$ (SH) and CdS/TiO$_2$ (SS)

CONCLUSIONS

1. Both CdS/TiO$_2$ (SH) and CdS/TiO$_2$ (SS) are able to facilitate photocatalytic degradation of lignin model compounds and kraft pine lignin at room temperature under a weak alkaline aqueous solution (pH=9.0) using a visible light source. During the photodegradation of kraft pine lignin under visible light irradiation, four monophenolic degradation products were detected, which were generated from the cleavage of the C$_\beta$-O bond and oxidation of the α-carbon or β-carbon. Compared to the other products, vanillin was the major product.

2. CdS/TiO$_2$ (SH) exhibited a much larger BET surface area, a stronger absorption intensity in the wavelength range of 400 nm and 500 nm, and a weaker peak of PL spectrum than CdS/TiO$_2$ (SS), resulting in higher photodegradation rates.

3. Both phenolic and non-phenolic lignin units are reactive, but phenolic units appear to react faster. Compared with previous UV or organic systems of lignin photodegradation, this aqueous and visible-light photodegradation system could result in higher solar resource utilization and less cost. However, only small amounts of degradation products can be isolated, probably because the degradation products could be easily photodegraded in the same reaction system. The photocatalytic selectivity needs to be improved to produce low molecular weight chemicals from lignin.

ACKNOWLEDGMENTS

bioresources.com

REFERENCES CITED

Alvira, P., Tomás-Pejó, E., Ballesteros, M., and Negro, M. J. (2010). "Pretreatment technologies for an efficient bioethanol production process based on enzymatic hydrolysis: A review," *Bioresource Technology* 101(13), 4851-4861. DOI: 10.1016/j.biortech.2009.11.093

Arnaudov, L., Denkov, N. D., Surcheva, I., Durbut, P., Broze, G., and Mehreteab, A. (2001). "Effect of oily additives on foamability and foam stability. 1. Role of interfacial properties," *Langmuir* 17(22), 6999-7010. DOI: 10.1021/la010600r

Beis, S. H., Mukkamala, S., Hill, N., Joseph, J., Baker, C., Jensen, B., Stemmler, E. A., Wheeler, M. C., Frederick, B. G., Van Heiningen, A., Berg, A. G., and DeSisto, W. J. (2010). "Fast pyrolysis of lignin," *BioResources* 5(3), 1408-1424. DOI: 10.15376/biores.5.3.1408-1424

Biannic, B., and Bozell, J. J. (2013). "Efficient cobalt-catalyzed oxidative conversion of lignin models to benzoquinones," *Organic Letters* 15(11), 2730-2733. DOI: 10.1021/ol401065r

Brebu, M., Tamminen, T., and Spiridon, I. (2013). "Thermal degradation of various lignins by TG-MS/FTIR and Py-GC-MS," *Journal of Analytical Applied Pyrolysis* 104, 531-539. DOI: 10.1016/j.jaap.2013.05.016

Buendia, J., Mottweiler, J., and Bolm, C. (2011). "Preparation of diastereomerically pure dilignol model compounds," *Chemistry - A European Journal* 17(49), 13877-13882. DOI: 10.1002/chem.201101579

Chen, W. H., Cheng, W. Y., Lu, K. M., and Huang, Y. P. (2011). "An evaluation on improvement of pulverized biomass property for solid fuel through torrefaction," *Applied Energy* 88(11), 3636-3644. DOI: 10.1016/j.apenergy.2011.03.040

Costa, J. C., and Alves, M. M. (2013). "Posttreatment of olive mill wastewater by immobilized TiO_2 photocatalysis," *Photochemical and Photobiological Science* 89(3), 545-551. DOI: 10.1111/php.12023

Fox, E. B., Liu, Z. W., and Liu, Z. T. (2013). "Ultraclean fuels production and utilization for the twenty-first century: Advances toward sustainable transportation fuels," *Energy and Fuels* 27(11), 6335-6338. DOI: 10.1021/ef401094t

Hartwig, J. F., Sergeev, A. G., and Webb, J. D. (2012). "A heterogeneous nickel catalyst for the hydrogenolysis of aryl ethers without arene hydrogenation," *Journal of the American Chemical Society* 134(50), 20226-20229. DOI: 10.1021/ja3085912

Higashimoto, S., Tanaka, Y., Ishikawa, R., Hasegawa, S., Azuma, M., Ohue, H., and Sakata, Y. (2013). "Selective dehydrogenation of aromatic alcohols photocatalyzed by Pd-deposited CdS-TiO_2 in aqueous solution using visible light," *Catalysis Science and Technology* 3(2), 400-403. DOI: 10.1039/C2CY20607B

Huo, Y., Yang, X., Zhu, J., and Li, H. (2011). "Highly active and stable CdS-TiO_2 visible photocatalyst prepared by in situ sulfurization under supercritical conditions," *Applied Catalysis B: Environmental* 106(1-2), 69-75. DOI: 10.1016/j.apcatb.2011.05.006

Larraufie, M. H., Pellet, R., Fensterbank, L., Goddard, J. P., Lacôte, E., Malacria, M., and Ollivier, C. (2011). "Visible-light-induced photoreductive generation of radicals from epoxides and aziridines," *Angewandte Chemie (International Edition)* 50(19), 4463-4466. DOI: 10.1002/ange.201007571

Li, D. Z., Chen, Z. X., Chen, Y. L., Li, W. J., Huang, H. J., He, Y. H., and Fu, X. Z. (2008). "A new route for degradation of volatile organic compounds under visible

light: Using the bifunctional photocatalyst Pt/TiO$_{2-x}$N$_x$ in H$_2$-O$_2$ atmosphere," *Environmental Science and Technology* 42(6), 2130-2135. DOI: 10.1021/es702465g

Ma, Y. S., Chang, C. N., Chiang, Y. P., Sung, H. F., and Chao, A. C. (2008). "Photocatalytic degradation of lignin using Pt/TiO$_2$ as the catalyst," *Chemosphere* 71(5), 998-1004. DOI: 10.1016/j.chemosphere.2007.10.061

Mali, S. S., Desai, S. K., Dalavi, D. S., Betty, C. A., Bhosale, P. N., and Patil, P. S. (2008). "CdS-sensitized TiO$_2$ nanocorals: Hydrothermal synthesis, characterization, application," *Photochemical and Photobiological Science* 10(10), 1652-1658. DOI: 10.1039/c1pp05084b

Melligan, F., Hayes, M. H. B., Kwapinski, W., and Leahy, J. J. (2012). "Hydro-pyrolysis of biomass and online catalytic vapor upgrading with Ni-ZSM-5 and Ni-MCM-41," *Energy and Fuels* 26(10), 6080-6090. DOI: 10.1021/ef301244h

Mohan, D., Pittman, C. U., and Steele, P. H. (2006). "Pyrolysis of wood/biomass for bio-oil: A critical review," *Energy and Fuels* 20(3), 848-889. DOI: 10.1021/ef0502397

Nah, Y. C., Paramasivam, I., and Schmuki, P. (2010). "Doped TiO$_2$ and TiO$_2$ nanotubes: Synthesis and applications," *ChemPhysChem* 11(13), 2698-2713. DOI: 10.1002/cphc.201000276

Nguyen, J. D., Matsuura, B. S., and Stephenson, C. R. J. (2013). "A photochemical strategy for lignin degradation at room temperature," *Journal of the American Chemical Society* 136(4), 1218-1221. DOI: 10.1021/ja4113462

Parsell, T. H., Owen, B. C., Klein, I., Jarrell, T. M., Marcuum, C. L., Haupert, L. J., Amundson, L. M., Kenttämaa, H. I., Ribeiro, F., Miller, J. T., and Abu-Omar, M. M. (2013). "Cleavage and hydrodeoxygenation (HDO) of C-O bonds relevant to lignin conversion using Pd/Zn synergistic catalysis," *Chemical Science* 4(2), 806-813. DOI: 10.1039/C2SC21657D

Peng, S. Q., Huang, Y. H., and Li, Y. X. (2013). "Rare earth doped TiO$_2$-CdS and TiO$_2$-CdS composites with improvement of photocatalytic hydrogen evolution under visible light irradiation," *Materials Science in Semiconductor Processing* 16(1), 62-69. DOI: 10.1016/j.mssp.2012.06.019

Qian, S., Wang, C., Liu, W., Zhu, Y., Yao, W., and Lu, X. (2011). "An enhanced CdS/TiO$_2$ photocatalyst with high stability and activity: Effect of mesoporous substrate and bifunctional linking molecule," *Journal of Materials Chemistry* 21(13), 4945-4952. DOI: 10.1039/C0JM03508D

Stärk, K., Taccardi, N., Bosmann, A., and Wasserscheid, P. (2010). "Oxidative depolymerization of lignin in ionic liquids," *ChemSusChem* 3(6), 719-723. DOI: 10.1002/cssc.200900242

Tuck, C. O., Pérez, E., Horváth, I. T., Sheldon, R. A., and Poliakoff, M. (2012). "Valorization of biomass: Deriving more value from waste," *Science* 337(6095), 695-699. DOI: 10.1126/science.1218930

Tucker, J. W., Narayanam, J. M. R., Shah, P. S., and Stephenson, C. R. J. (2011). "Oxidative photoredox catalysis: Mild and selective deprotection of PMB ethers mediated by visible light," *Chemical Communication* 47(17), 5040-5042. DOI: 10.1039/c1cc10827a

Voitl, T., Nagel, M. V., and von Rohr, P. R. (2010). "Analysis of products from the oxidation of technical lignins by oxygen and H$_3$PMo$_{12}$O$_{40}$ in water and aqueous methanol by size-exclusion chromatography," *Holzforschung* 64(1), 13-9. DOI: 10.1515/hf.2010.006

Wang, J., Liu, Z., Zheng, Q., He, Z. K., and Cai, R. X. (2006). "Preparation of photosensitized nanocrystalline TiO_2 hydrosol by nanosized CdS at low temperature," *Nanotechnology* 17(18), 4561-4566. DOI: 10.1088/0957-4484/17/18/006

Wu, A., Patrick, B. O., Chung, E., and James, B. R. (2012). "Hydrogenolysis of β-O-4 lignin model dimers by a ruthenium-xantphos catalyst," *Dalton Transactions* 41(36), 11093-11106. DOI: 10.1039/c2dt31065a

Zakzeski, J., Bruijnincx, P. C. A., Jongerius, A. L., and Weckhuysen, B. M. (2010). "The catalytic valorization of lignin for the production of renewable chemicals," *Chemical Reviews* 110(6), 3552-3599. DOI: 10.1021/cr900354u

Zhang, X. H., Zhang, Q., Long J. X., Xu, Y., Wang, T. J., Ma, L. L., and Li, Y. P. (2014). "Phenolics production through catalytic depolymerization of alkali lignin with metal chlorides," *BioResources* 9(2), 3347-3360. DOI: 10.15376/biores.9.2.3347-3360